Research Article

R. Bouchenafa* and H. A. Mohammed

Numerical study of the thermal and hydraulic performances of heat sink made of wavy fins

https://doi.org/10.2478/mme-2019-0021
Received Feb 12, 2018; revised Sep 1, 2018; accepted Nov 20, 2018

Abstract: The aim of this paper is to numerically investigate the thermal and hydraulic performances of the two heat sinks made of wavy fins (WFHS). The governing equations fitted with boundary conditions were solved using the finite volume method, and the SIMPLE algorithm for the coupling velocity-pressure. The two-equation model k-ϵ was used to describe the turbulence phenomenon. The effects of wave numbers and the amplitude of wavy fins heat sink on the thermal and flow fields are studied and compared with the plate fin heat sink (PFHS). The results show that the use of wavy fins improves significantly the heat transfer rate, accompanied by a pressure drop penalty.

Keywords: Heat transfer, heat sink, turbulent flow, wavy fins

1 Introduction

Currently, the power components, such as microprocessors, hard drives, memory modules, voltage converters and so on, can dissipate heat measuring up to several hundred watts per square centimeter. The overheating of components reduces their lifespan and can cause operational constraints. Therefore, good heat dissipation is crucial to ensure the functioning and reliability of these devices. To maintain a nominal operating temperature, the implementation of an effective cooling system and heat dissipation is necessary. Because of its simplicity, facility of implementation and low cost, forced and natural convection of air through the heat sink is the most commonly used method for cooling the electronic components.

In this context, several experimental and numerical works have been published in the literature. Hung *et al.* [1] measured the heat sinks' thermal performance cooled by a jet impact using infrared thermography. Thermal resistance was analyzed as a function of the impinging Reynolds number, the width and height of the fins, the distance between the nozzle and the tip of the fins, and the type of heat sinks. The results show that by increasing the Reynolds number, the width and height of the fins always reduce the thermal resistance. Thermal performance of plate fins and pin fins heat sinks commonly used in the electronics industry was compared experimentally by Dong *et al.* [2, 3] The experiments were carried out for various flow rates and channel widths. From the experimental data, a model based on the finite volume method for predicting the pressure drop and the thermal resistance was suggested. By comparing the two types of heat sinks, pins fins heat sink were found to have a lower thermal resistance.

Shaeri and Yaghoubi [4] proposed a three-dimensional numerical study of forced convective heat transfer from a row of solid and perforated fins mounted on a flat wall. The Navier-Stokes equations based on k-ϵ (RNG) turbulence model were solved by the finite volume method and SIMPLE algorithm. For a range of Reynolds number between 2 x 104 and 4 x 104 and for Prandtl number Pr = 0.71, the results show that the heat transfer is more important in the case of perforated fins. Kok-Cheong and Sanjiv [5] numerically studied the profile's effect on the flow and thermal characteristics between the plate fins. The results indicate that the U-shaped profile improves the overall thermal efficiency. In order to improve the performance of a plate fin heat sink fitted with two vortex generators, Hung *et al.* [6] studied the effects of the distance between the vortex generators and the heat sink, the distance between the vortex generators, and the angle of incidence and height of generators. The results show that the angle of incidence of 30° is preferable to optimize the pressure drop and thermal resistance. The performance of a commercial heat sink composed with corrugated walls

***Corresponding Author: R. Bouchenafa:** UFR Sciences et Techniques, Université du Havre, France, 25 rue Philippe Lebon - BP 1123 - 76063 Le Havre Cedex France; Email: rachid.bouchenafa@etu.univ-lehavre.fr
H. A. Mohammed: Department of Energy Engineering, Technical College of Engineering, Duhok Polytechnic University (DPU), 61 Zakho Road, 1006 Mazi Qr, Duhok-Kurdistan Region, Iraq

was experimentally investigated by Marco *et al.* [7] The influences of the heat flow imposed (uniform and non-uniform) and the space between the heat sink and the fan were examined. The velocity distribution in the channels and the overall thermal resistance were presented and analyzed. The results indicate that the device is more efficient when the heat source is distributed over the whole surface of the heat sink, and in this case, decreasing the number of spacers brings a decrease in the thermal resistance. Roody and Chi [8] have made a comparative study of heat sinks having different shapes under natural convection mode. The pattern comprises rectangular, trapezoidal and reversed trapezoidal fins. From the test results, the heat transfer coefficient of conventional rectangular fins was greater than that of the trapezoidal fins, while the heat transfer coefficient of inverted trapezoidal fins was greater than the trapezoidal and rectangular fins about 25% and 10% respectively. Mahmoud *et al.* [9] studied experimentally the effects of micro fin height (0.25 to 1.0 mm) and spacing (0.5 to 1.0 mm) on the heat transfer coefficient for a heat sink mounted horizontally with natural convection conditions. The results show that the heat transfer coefficient by convection increased with increasing the spacing between the fins, and decreased with increasing the fins height.

A comparative study of heat sinks having different shapes under natural convection mode was also carried out by Pankaj and Anil. [10] The pattern comprises vertical fins, horizontal fins and an upwardly shaped configuration. They concluded that the cooling of high power and large-scale systems requires a higher thermal dissipation. Razavi *et al.* [11] made a numerical study of the hydro thermal energy in a new plate-pin fins heat sink by using a thin plate known as a separator attached to the pin fin. The results show that to reduce the thermal resistance and pressure drop, the thin plate must be put behind the pin fin. The effects of duct height, duct width, fin height, fin width, fin-to-fin distance and Reynolds number on the performance of the heat sinks are examined by Jonsson and Moshfegh. [12] They considered the bypass effect of seven types of heat sinks plate-fin, in-line strip-fin, staggered strip-fin, in-line circular pin-fin, staggered circular pin-fin, in-line square pin-fin and staggered square pin-fin. The Reynolds number and the relative duct height are the dominating parameters for the Nusselt number.

Xiaoling *et al.* [13] compared the thermal performance of two kinds of heat sinks such as plate fin heat sink and plate-pin fin heat sink. A constant heat flux of 10 W was applied on the base of the heat sinks and the air velocity was varied from 6.5 m/s to 12.2 m/s. They observed that the plate pin fin heat sink gives a lower thermal resistance and more pressure drop than the plate fin heat sinks.

Similarly, Yue *et al.* [14] studied and compared numerically the thermal and hydraulic performances of plate fin heat sink and pin fin heat sink. The results show that the heat transfer performance increased sharply with the increase of the air velocity especially for pin fin heat sinks. Hung and Ming-Hung [15] investigated the effects of a shield on the thermal and hydraulic characteristics of plate-fin vapor chamber heat sinks under cross flow cooling. The infrared thermography technique was used to measure the temperature. The thermal-fluid performance of vapor chamber heat sinks with a shield was studied as a function of the Reynolds number, fin height and fin width. By comparing with those without a shield, the maximum surface temperature of the vapor chamber heat sink is effectively reduced.

Similarly, Mohamed *et al.* [16] investigated experimentally and numerically the effect of shield inclination (θ = 30° to θ = 150°) on the thermal and hydraulic performance of plate fin heat sink. It was found that the thermal resistance is minimum when the shield inclination varied between 90° and 120° and for the shortest fin height. Mohamed and Osama [17] extended the previous study by making a different number of slots in the shield at different positions. The thermal resistance and pressure drop were investigated as a function of the Reynolds number, slot width and slots number. It was found that the use of the slotted shield enhances the flow performance and can reduce the pressure drop by about 80% as compared with the solid shield. Yuan [18] studied the effect of the width and height of a rectangular channel on the performance of a plate fins heat sink using Fluent CFD code. The numerical results are verified by comparison with an experimental test model. The results showed that the air flow enters the fin to fin passage and decelerates with distance downstream; thus, influencing the effect of heat transfer.

Sam *et al.* [19] studied the heat transfer characteristics of heat sink with continuous and interrupted rectangular fins. They provided through holes on both the rectangular fins and observed that the interrupted fin with through holes gives a better performance than the interrupted rectangular fins of heat sinks. Lei *et al.* [12] studied numerically the characteristics of laminar flow and heat transfer in micro-channel heat sink with offset ribs on the side walls. Five forms of compensation ribs were designed – rectangular, backward triangular, isosceles triangular, forward triangular and semicircular – with the Reynolds number varying between 190 and 838. They found that the heat transfer is more significant in the forward triangular ribs for Re < 350, and for Re > 400 the semicircular ribs

Table 1: Heat sinks dimensions

h (*mm*)	n = 2	n = 3	n = 5	L (*mm*)	H (*mm*)	S (*mm*)	t (*mm*)
2	δ = 25.5 mm	δ = 17 mm	10.2 mm	51	10	5	1.5
3	δ = 25.5 mm	δ = 17 mm	10.2 mm	51	10	5	1.5
4	δ = 25.5 mm	δ = 17 mm	10.2 mm	51	10	5	1.5

have the best performance. Ismail *et al.* [21] carried out a numerical and experimental investigation on the corrugation profile effect on the thermal-hydraulic performance of the micro-channel heat sinks. Three forms of roughness – sinusoidal, triangular and trapezoidal – were examined. They concluded that the use of a corrugated channel is an appropriate method for increasing the thermal efficiency and to obtain a higher capacity of the heat sink. Kavita *et al.* [22] studied experimentally the usage of square and circular perforated plate fin arrays under forced convection condition. The perforation size varied as 6 mm, 8 mm and 10 mm, and the Reynolds number varied from 2.1×10^4 to 8.7×10^4. They observed that the square perforated fin array gives more heat transfer at a low Reynolds number and the circular perforated fin array performs better at a high Reynolds number.

From the above literature review, many researchers have investigated the thermal and dynamic performances of plate fins heat sink, by the combination of plate and pins fins, the insertion of shields on bypass, the use of fins with rough walls and the perforation of the fins. However, in this numerical study, a new model of heat sink made of wavy fins was suggested to enhance the heat transfer as compared with the plate fins heat sink.

2 Geometry and mathematical model

2.1 Problem definition

The geometry of the considered problem is shown in Figure 1. The physical model is based on the work published by Yuan *et al.* [22] It is a heat sink made of plate fins (Figure 1(a)) and wavy fins (Figure 1(b)). The details of the wavy fins are illustrated in Figure 1(c). The geometrical parameters are listed in Table 1.

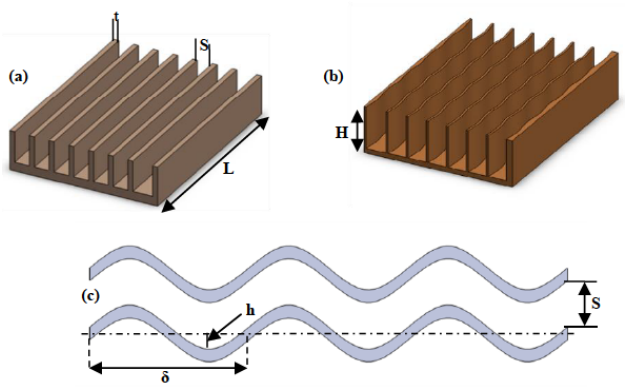

Figure 1: Schematic diagrams of heat sinks: a) Plate fin heat sink, b) Wavy fin heat sink, c) Details of wavy fins

2.2 Governing equations

In this work, the fluid is assumed to be incompressible and the flow is turbulent, three-dimensional and steady state. The effects of radiation heat transfer and buoyancy are neglected. The governing equations are as follows (Feng and Ivan [23]):

2.2.1 Continuity equation:

$$\frac{\partial \rho u_i}{\partial x_i} = 0 \tag{1}$$

2.2.2 Momentum equation:

$$\rho u_j \frac{\partial u_i}{\partial x_j} = \frac{\partial}{\partial x_j}\left[(\mu + \mu_t)\frac{\partial u_i}{\partial x_j}\right] - \frac{\partial P}{\partial x_i} = 0 \tag{2}$$

2.2.3 Energy equation:

$$\rho u_j \frac{\partial T}{\partial x_j} = \frac{\partial}{\partial x_j}\left[\left(\frac{\mu}{\mathrm{Pr}} + \frac{\mu_t}{\mathrm{Pr}_t}\right)\frac{\partial T}{\partial x_j}\right] = 0 \tag{3}$$

2.3 Turbulence model

The k–ω model is defined by two transport equations, one for the turbulent kinetic energy (k) and the other for the specific dissipation rate (ϵ), as given below (Lauder and Spalding [24]):

$$\frac{\partial}{\partial x_i}(\rho k u_i) = \frac{\partial}{\partial x_j}\left[\left(\mu + \frac{\mu_t}{\sigma_t}\right)\frac{\partial k}{\partial x_j}\right] + G_k - \rho\varepsilon = 0 \quad (4)$$

$$\frac{\partial}{\partial x_i}(\rho\varepsilon u_i) = \frac{\partial}{\partial x_j}\left[\left(\mu + \frac{\mu_t}{\sigma_{kt}}\right)\frac{\partial \varepsilon}{\partial x_j}\right] + C_1\frac{\varepsilon}{k}G_k - C_{2\varepsilon}\frac{\varepsilon^2}{k} = 0 \quad (5)$$

where G_k is the rate of generation of the TKE, while $\rho\ \epsilon$ is its destruction rate. G_k is written as:

$$G_k = -\rho\overline{u_i' u_j'}\frac{\partial u_j}{\partial x_i} \quad (6)$$

The empirical constants for the turbulence model are arrived at by comprehensive data fitting for a wide range of turbulent flow.

$C_\mu = 0.09$, $C_{\epsilon 1} = 1.47$, $C_{\epsilon 2} = 1.92$, $\sigma_k = 1.0$, $\sigma_\epsilon = 1.3$

2.4 Computational domain and boundary conditions

The computational domain fitted with boundary conditions of this study are presented in Figure 2. The base of heat sink is maintained at a constant heat flux (Q), and the extended walls are adiabatic. At the inlet, the fluid enters the channel with a uniform velocity and uniform temperature. At the outlet, the flow may safely be assumed as fully-developed, which implies negligible stream wise gradients of all variables.

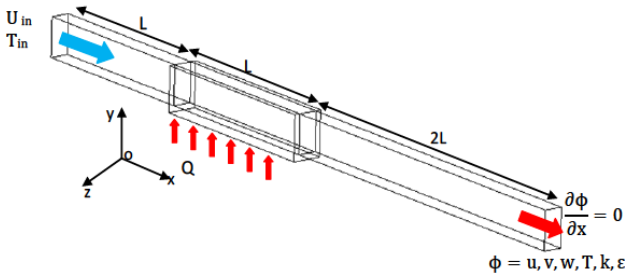

Figure 2: Computational domain and boundary conditions

2.5 Characteristic parameters

2.5.1 Average Nusselt number is defined as:

$$Nu_m = \frac{hD_h}{\lambda_f} \quad (7)$$

where the hydraulic diameter D_h is calculated as:

$$D_h = \frac{4A}{P} = \frac{4 \times H \times S}{2(H+S)} \quad (8)$$

2.5.2 Reynolds number is defined as:

$$\mathrm{Re} = \frac{u_{in}D_h}{\nu_f} \quad (9)$$

where υ_f is the kinematic viscosity.

2.5.3 Pressure drop is defined as:

$$\Delta P(x) = P_{in} - P_{out} \quad (10)$$

2.5.4 Thermal resistance is defined as:

$$R_{th} = \frac{\Delta T}{Q} \quad (11)$$

where $\Delta T = T_{b\,\max} - T_{in}$

T_{bmax} - Maximum temperature of the heat sink base (K)

T_{in} - Inlet air temperature (K)

2.6 Numerical solution

The commercial computer code FLUENT is used to calculate the fluid flow and heat transfer in the computational domain. The governing equations provided with boundary conditions are solved using the finite volume method based on the SIMPLE algorithm (Patankar, [25] Doormal and Raithby [26]). Both solid and fluid phases were simultaneously solved as a single domain. Momentum and energy equation are approximated with the second order upwind differencing scheme. The solutions were considered to be converged when the convergence criterion values hit 10^{-6} for all variables.

2.6.1 Grid sensitivity

A serial of test simulations (Nx-Ny-Nz) were performed to ensure the grid independence for an inlet velocity equal to 10m/s (Re = 5300).

- Plate fin heat sink (PFHS): The mesh densities of (280 × 62 × 59), (240 × 55 × 50), (200 × 43 × 41), (160 ×x31 ×27), and (120 × 19 × 18) were used.
- Wavy fin heat sink (WFHS) having (n = 3 and h = 3 mm): The mesh densities of (320 × 74 × 68), (280 × 62 × 59), (240 × 55 × 50), and (200 × 43 × 41) were used.

Figures 3 and 4 represent the variation of axial velocity in a section x = 0.0255 m for different grids applied on both types of heat sinks. The velocities' profiles correspond to the mesh (240 × 55 ×50) and (280 × 62 × 59) for PFHS, (280 × 62 × 59) and (320 × 74 × 68) for WFHS are almost confounded and with slight difference. To minimize the time of calculation, the mesh (240 × 55 × 50) for PFHS and the mesh (280 × 62 × 59) for WFHS were adopted to perform the simulations.

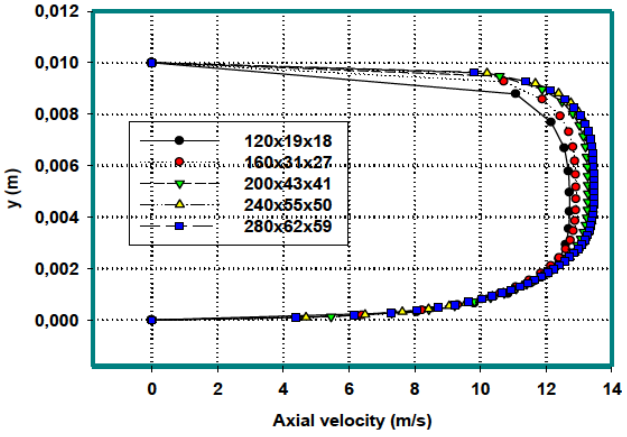

Figure 3: Influence of the mesh on the axial velocity for plate fin heat sink

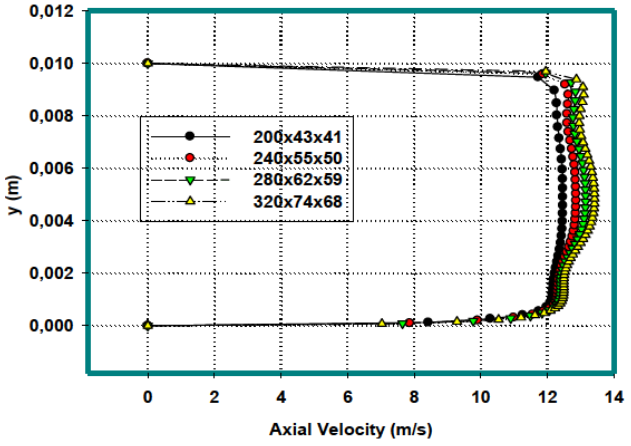

Figure 4: Influence of the mesh on the axial velocity for wavy fin heat sink

2.6.2 Model validation

Figure 5 shows a comparison of the present results with the results obtained by Xiaoling *et al.* [12] In this figure, the variation of thermal resistance with inlet velocities is presented. It is clear that the results are in a good agreement, which allowed us to study the problem numerically.

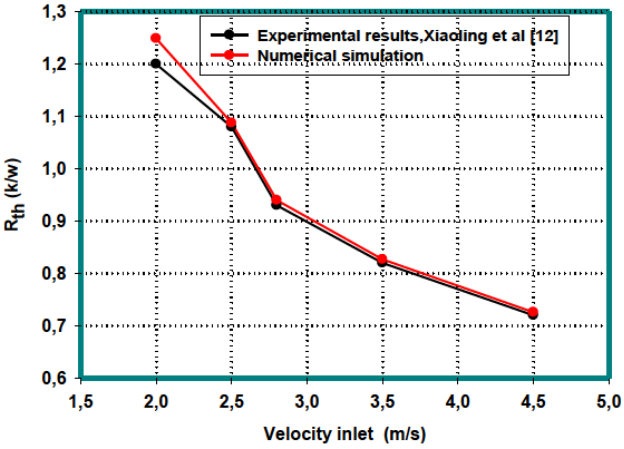

Figure 5: Comparison of the present results with the experimental study of Xiaoling *et al.* [12]

3 Results and discussion

3.1 Hydraulic Characteristics

3.1.1 Flow fields distribution

Figures 6 and 7 present an example of the axial velocity fields for plate and wavy fins heat sinks, within a plane y = 0.005 m and for a Reynolds number equal to 5300, which corresponds to an inlet velocity equal to 10 m/s.

For wavy heat sinks, it can be seen that the maximum velocities in convex summits and negative velocities in the concave tops. On the other hand, in the plate fin heat sink, the air velocity is maximum at the center. The increase of wave numbers and the amplitude causes an acceleration of the air to the convex vertices to have the velocities of around 22 m/s (n = 5) and 20 m/s (h = 4 mm). In the concave summits, the negative velocities also increase and reach the values of around −2 (m/s) (n = 5 and h = 4 mm).

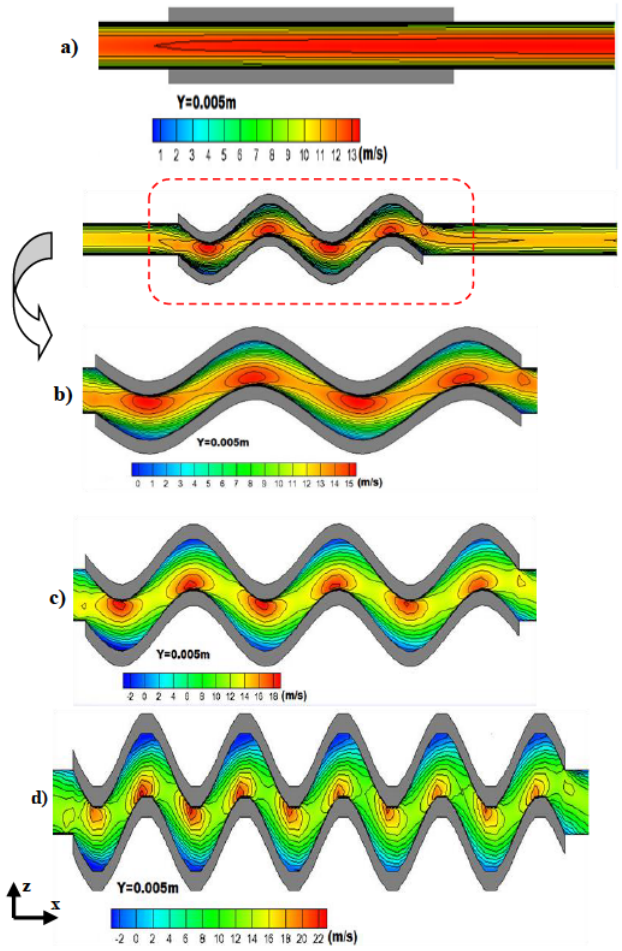

Figure 6: Axial velocity contours (h = 3mm),: a) PFHS, b) n = 2, c) n = 3, d) n = 5

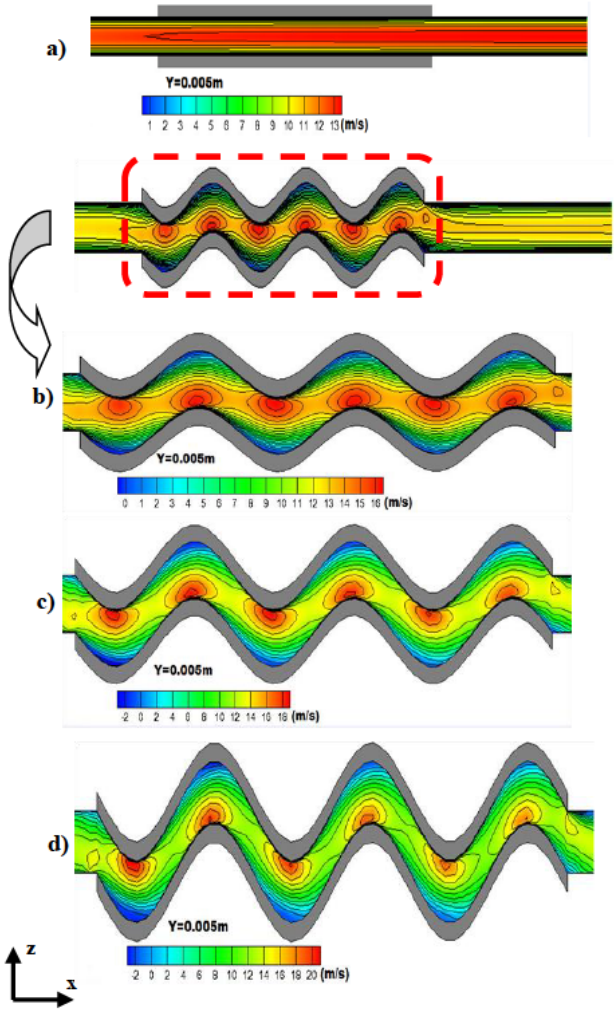

Figure 7: Axial velocity contours (n = 3): a) PFHS, b) h = 2 mm, c) h = 3 mm, d) h = 4 mm

3.1.2 Velocity profiles in different sections of heat sinks

Analysis of the flow through the heat sinks is much clearer on the velocity profiles. Figure 8 shows the different sections chosen, namely x = 0.0255 m (y = 0.005 m), x = 0.02975 m (y = 0.005m) for plate and wavy heat sinks (n = 2 ; n = 3 ; n = 5 et h = 3 mm), (h = 2 mm ; h = 3 mm ; h = 4 mm et n = 3).

Figures 9 and 10 show the variation of the axial velocity in two selected sections at x = 0.0255 m and x = 0.02975 m, for a heat sink having three waves and an amplitude equal to 3 mm. It clearly appears that the velocity profiles take a parabolic shape for the two heat sinks. In half of the domain (at x = 0.0255 m), the air velocity has the maximum values at the center of the flow. This velocity decreases related to the walls. In the section (x = 0.02975 m) that corresponds to both convex and concave summits (Figure 9), it is noted that the velocities are proportional as a function of the amplitude. The appearance of negative velocities in the concave summits signified the presence of air recirculation zones.

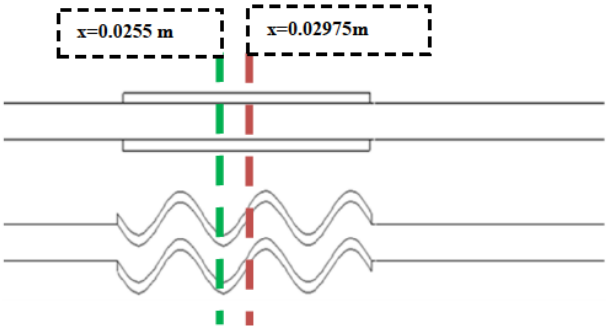

Figure 8: Selected sections

Table 2: Percentages of pressure drop in WFHSs compared to PFHS

WFHS	n = 5			h = 4 mm		
	h = 2 mm	h = 3 mm	h = 4 mm	n = 2	n = 3	n = 5
[%]	89 %	96 %	98%	28%	89%	98%

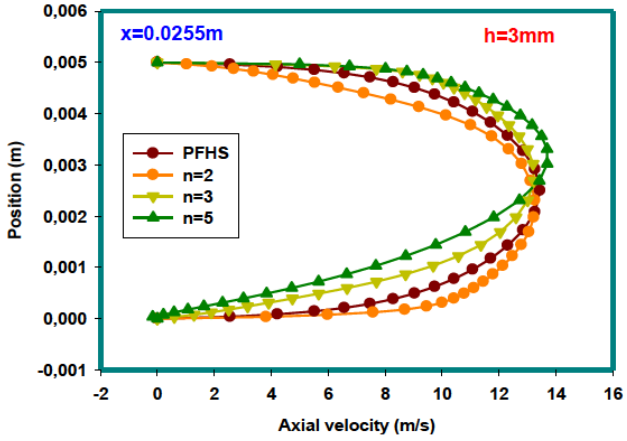

Figure 9: Variation of axial velocity in the section x = 0.0255 m

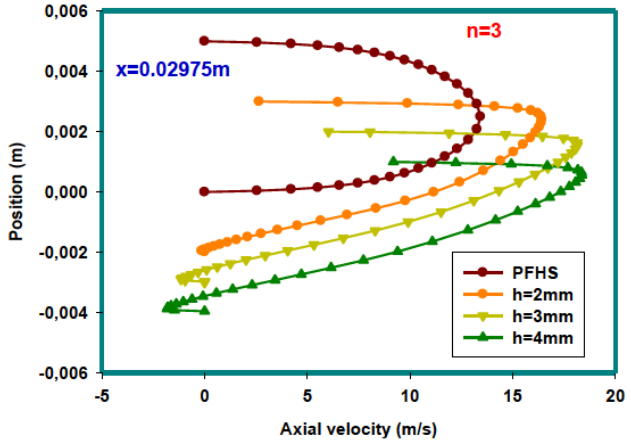

Figure 10: Variation of axial velocity in the section x = 0.02975 m

3.1.3 Pressure drop

The pressure losses according to the air velocity for different heat sinks are shown in Figures 11 and 12. It can be seen that the pressure drops vary proportionally with the air inlet velocity, the number of waves (n) and the amplitude (h).

Comparisons of the pressure drop are shown in Table 2. The WFHS (h = 4 mm, n = 5) has a pressure loss of about 98% higher than the PFHS, while the WFHSs (h = 2 mm; n = 5) and (n = 3; h = 4 mm) have a similar pressure drop of about 89%. This is attributed to the higher friction and blockage effect associated with increasing Reynolds number.

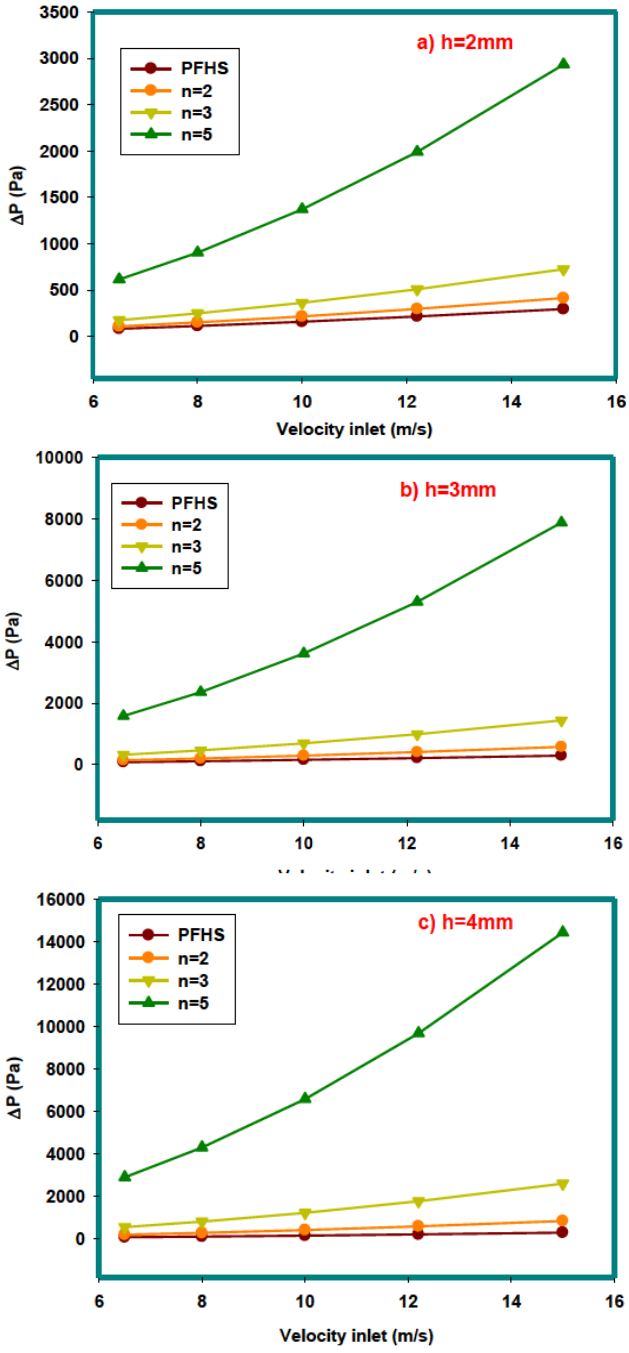

Figure 11: Variation in pressure drop as a function of air velocity and wave number: a) h = 2 mm, b) h = 3mm, c) h = 4mm

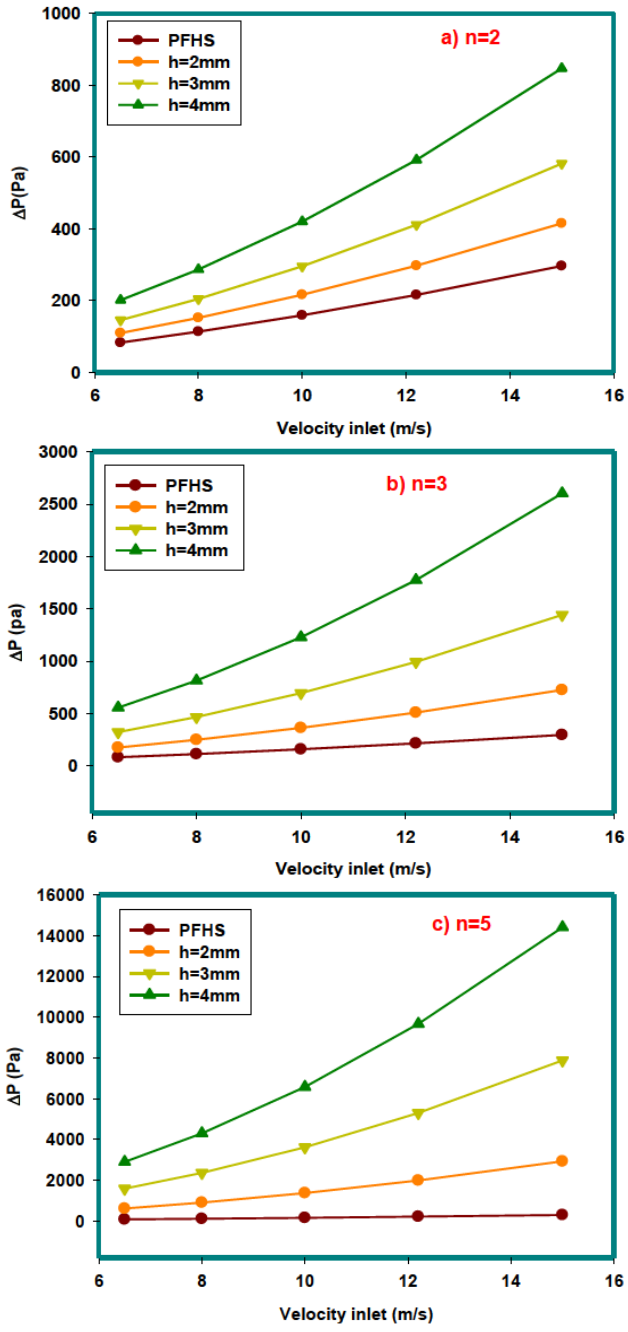

Figure 12: Variation in pressure drop as a function of velocity and amplitude: a) n = 2, b) n = 3, c) n = 5

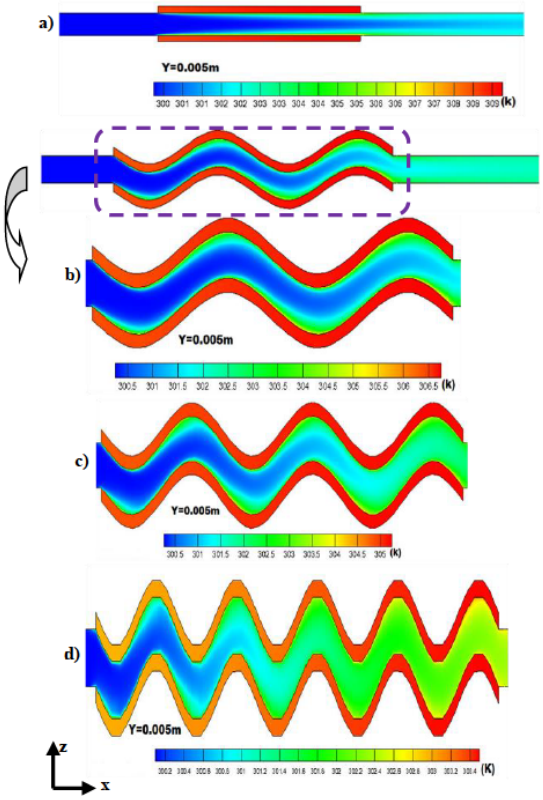

Figure 13: Total temperature contours (h = 3mm): a) PFHS, b) n = 2, c) n = 3, d) n = 5

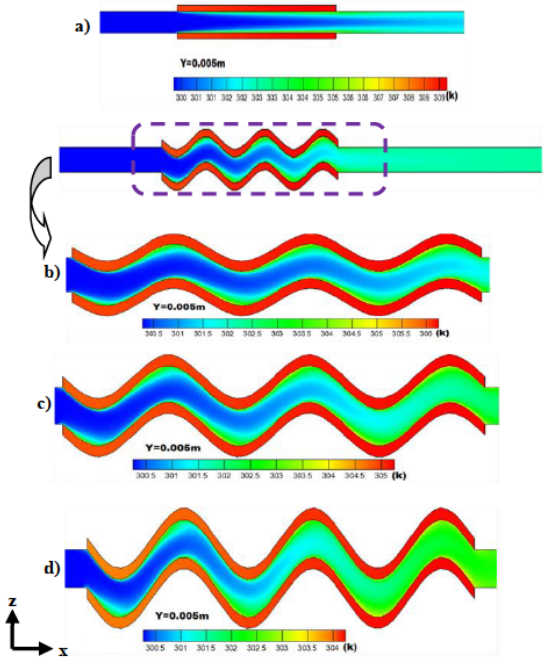

Figure 14: Total temperature contours, (n = 3): a) PFHS, b) h = 2 mm, c) h = 3 mm, d) h = 4 mm

3.2 Thermal Characteristics

3.2.1 Total temperature contours

Figures 13 and 14 show the distribution of the total temperature in the PFHS and WFHS, where the base is subjected to a constant heat flux. It can be seen that the fluid begins to heat up on contact with the hot walls. The temperature of the fluid increases gradually and reaches peak values at

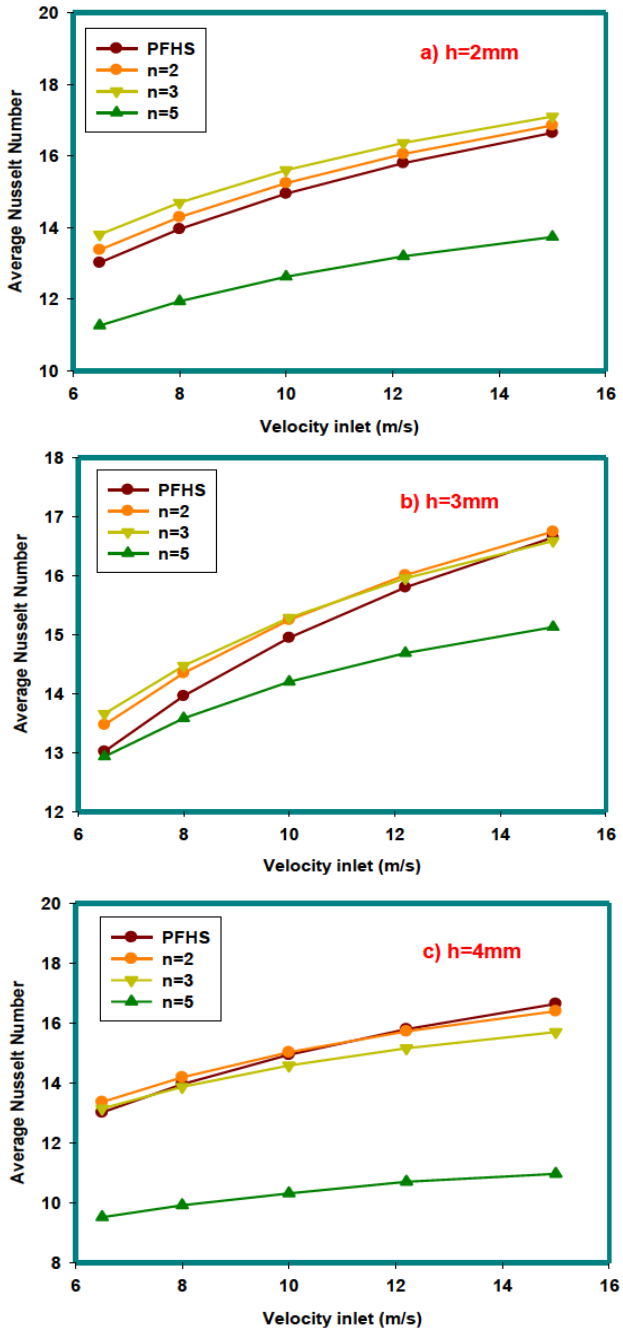

Figure 15: Average Nusselt number as a function of air velocity and wave number: a) h = 2 mm, b) h = 3 mm, c) h = 4 mm

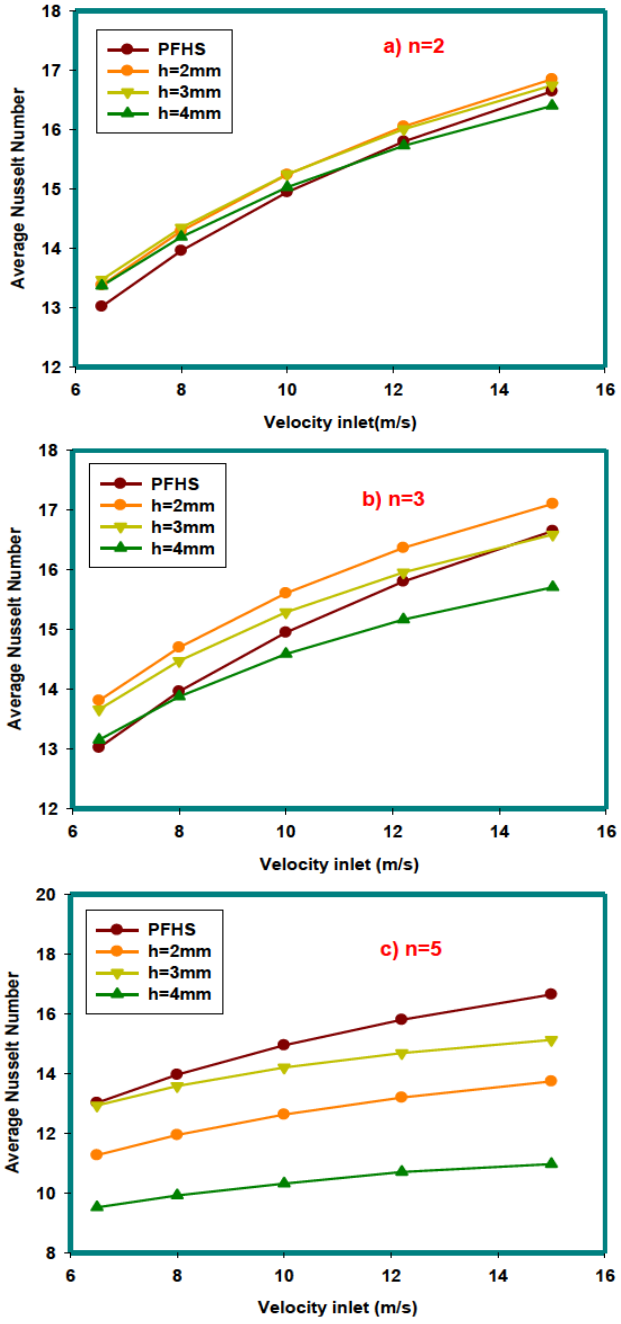

Figure 16: Average Nusselt number as a function of air velocity and amplitude: a) n = 2, b) n = 3, c) n = 5

the output. An increase in the wave number and the amplitude increases the trajectory and the air dwell time, which allows the absorption heat and cools the heat sinks.

3.2.2 Average Nusselt number

The evolution of the average Nusselt number as a function of the velocity of the air for the wavy fins heat sink are presented and compared with the plate fins heat sink in Figures 15 and 16. In all the cases, the Nusselt number increases with the velocity of air, the number of waves and the amplitude. For a wave number and an amplitude equal

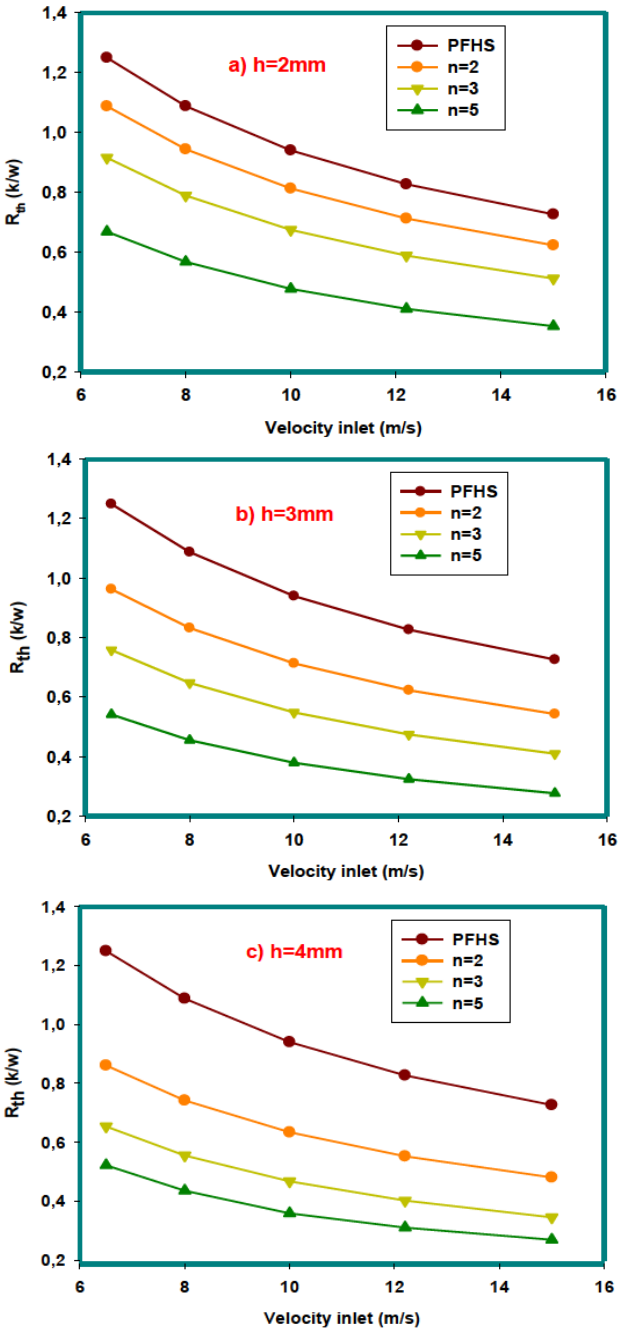

Figure 17: Thermal resistance as a function of air velocity and wave number: a) h = 2 mm, b) h = 3 mm, c) h = 4mm

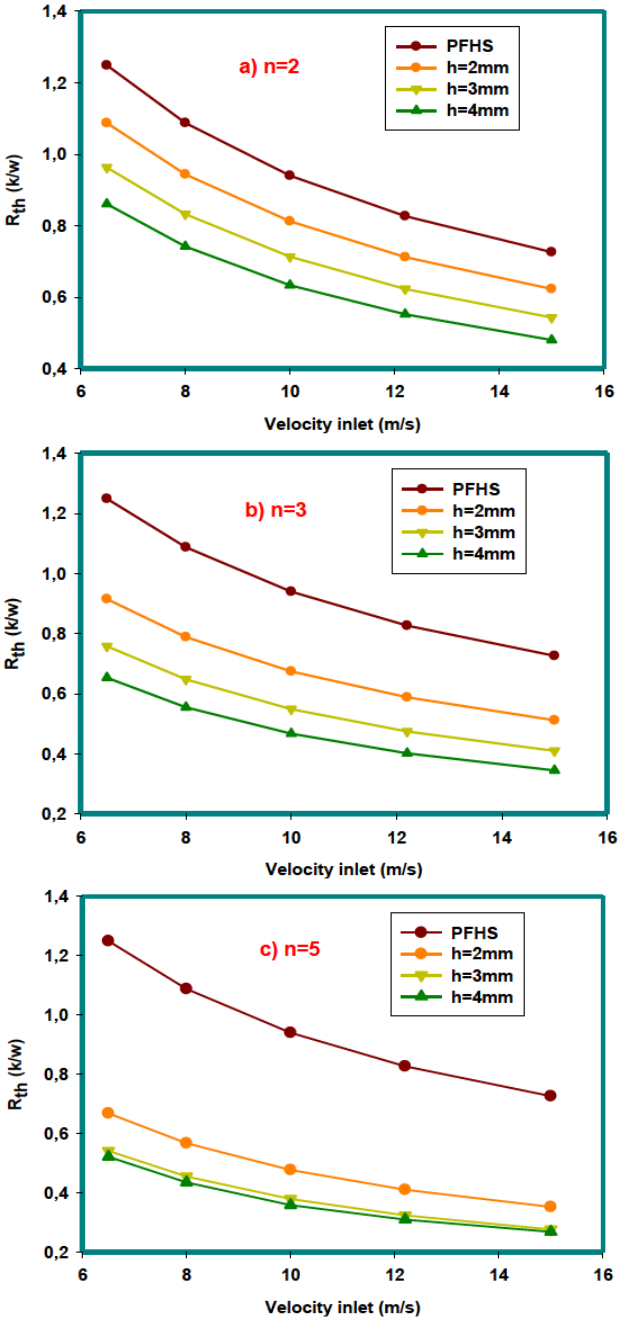

Figure 18: Thermal resistance as a function of air velocity and amplitude: a) n = 2, b) n = 3, c) n = 5

to two (Figures 15(a) and 16(a)), the convective heat transfer is relatively almost the same as the case of a plate fins heat sink. By increasing the number of waves and the amplitude, it can be noted that the convective heat transfer becomes large and reaches the highest values in the case of a heat sink composed of five waves and amplitude equal to 4 mm. This improvement in heat transfer is a result of the increase of the exchange surface. In addition, when h and n increases, the heat exchange surface would increase and eventually the heat transfer would also increase.

3.2.3 Thermal resistance

Thermal resistance results versus velocity are shown in Figures 17 and 18. It is clearly seen that thermal resistance is inversely proportional to air velocity. It is also noticed

that the plate fin heat sink has the highest thermal resistance as compared to the wavy fins heat sinks. By increasing the number of waves and the amplitude, the heat transferred to the air increases, and consequently, the maximum temperature of the heat sink base decreases, which results in a decrease in the thermal resistance. The heat sink that is composed of five waves and having an amplitude equal to 4 mm has the lowest thermal resistance compared with the other heat sinks. Besides, by using Equation (11), when h and n increases, the ΔT would decrease and then the Tb_{max} would decrease and this would result in R_{th} decrement.

4 Conclusions

A numerical investigation was carried out to study the turbulent flow of air through a wavy heat sink. The effects of wave number and amplitude on the hydraulic and thermal fields (pressure drop and average Nusselt number) were presented and analyzed. The governing partial differential equations were solved using the finite volume formulation along with the SIMPLE algorithm. The following conclusions can be drawn from the results:

- The heat sinks with wavy fins have a significant pressure drop with respect to plate fins heat sinks, due the increase of friction between the fluid and solid walls.
- The use of wavy fins increases the heat transfer significantly compared to plate fins.
- The lowest thermal resistance corresponds to the heat sink having the higher number of waves and the greatest amplitude.

References

[1] Hung, Y. L., Chao, S. M. and Tsai, G. L.: Thermal performance measurement of heat sinks with confined impinging jet by infrared thermography, Int. J. Heat Mass Transf. 48, 2005, 5386–5394.

[2] Kim, S. J., Dong, K. K and Oh, H. H. : Comparison of Fluid Flow and Thermal Characteristics of Plate-Fin and Pin-Fin Heat Sinks Subject to a Parallel Flow , Heat Transf. Eng. 29(2), 2008,169–177.

[3] Dong, K. K., Kim, S. J. and Bae, J. K.: Comparison of thermal performances of plate-fin and pin-fin heat sinks subject to an impinging flow, Int. J. Heat Mass Transf. 52,2009, 3510–3517.

[4] Shaeri, M. R., Yaghoubi, M.: Numerical analysis of turbulent convection heat transfer from an array of perforated fins, Int. J. Heat Fluid Flow 30, 2009, 218–228.

[5] Cheong, W. K., Sanjiv, I.: Impingement heat transfer of a plate fin heat sink with fillet profile, Int. J. Heat Mass Transf. 65, 1–9, 2013.

[6] Hung Y. L., Chen C., Chao S. M. and Liang G. F.: Enhancing heat transfer in a plate-fin heat sink using delta winglet vortex generators, Int. J. Heat Mass Transf. 67, 2013, 666–677.

[7] Marco L., Fabbri G., and Salvigni S.: Performance evaluation of a wavy-fin heat sink for power electronics, Appl. Therm. Eng. 27, 2007, 969–975.

[8] Roody, C., Chi, W.: A novel heat dissipation fin design applicable for natural convection augmentation, Int. Commun. Heat Mass Transf, 59, 2014, 24–29.

[9] Mahmoud, S., Al-Dadah R., Aspinwall D. K., Soo S. L. and Hemida H.: Effect of micro fin geometry on natural convection heat transfer of horizontal microstructures, Appl. Therm. Eng. 31, 2011, 627–633.

[10] Pankaj S., Anil K. P.: Experimental investigation of heat transfer enhancement through embossed fin heat sink under natural convection, Exper. Therm. Fluid Sci. 61, 2015, 24–33.

[11] Razavi S. E., Osanloo B., and Sajedi R.: Application of splitter plate on the modification of hydro-thermal behavior of PPFHS, Appl. Therm. Eng, 80, 2015, 97–108.

[12] Xiaoling Y., Feng J., Feng Q. and Wang Q.: Development of a plate-pin fin heat sink and its performance comparisons with a plate fin heat sink, Appl. Therm. Eng, 25, 2005, 173–182.

[13] Yang Y. T., Peng H. S.: Investigation of planted pin fins for heat transfer enhancement in plate fin heat sink, Microelectronics Reliability, 49, 2009, 163–169.

[14] Li H. Y., Chiang M. H.: Effects of shield on thermal-fluid performance of vapor chamber heat sink, Int. J. Heat Mass Transf. 54, 2011, 1410–1419.

[15] Mohamed R. S., Saleh M. A., Mesalhy O., and Elsayed M. L.: Thermo/fluid performance of a shielded heat sink, Int. J. Therm. Sci, 60, 2012, 171–181.

[16] Elsayed M. L., Osama M.: Effect of a Slotted Shield on Thermal and Hydraulic Performance of a Heat Sink, J. Elec. Packag, 137(1), 2014, 011004.

[17] Yuan T. D.: Computational modeling of flow bypass effects on straight fin heat sink in a rectangular duct, Twelfth IEEE Semitherm Symposium, 1996, 164–168.

[18] Sam S., Sriharsha G., Arun S. B., Kumar D. P. and Naidu C. S.: Modelling and Analysis of Heat Sink with Rectangular Fins Having Through Holes, Int. J. Eng. Res. and App, 3(2), 2013, 1557–1561.

[19] Lei C., Xia G. D. and Wang H. S.: Numerical study of laminar flow and heat transfer in microchannel heat sink with offset ribs on sidewalls, Appl. Therm. Eng, 92, 2016, 32–41.

[20] Ismail M. A., Abdullah M. Z. and Mujeebu M. A. : A CFD-based experimental analysis on the effect of free stream cooling on the performance of micro processor heat sinks, Int. Commun. Heat Mass Transf, 35, 2008, 771–778.

[21] Kavita H. D., Sunnapwar K. V. and Dhanawade H. S.: Thermal Analysis of Square and Circular Perforated Fin Arrays by Forced Convection, Int. J. Curr. Eng. Tech., Special Issue (2) 2014.

[22] Yuan W., Zhao J., Tso C.P., Tianhua W., Wei L. and Tingzhen M.: Numerical simulation of the thermal hydraulic performance of a plate pin fin heat sink, Appl. Therm. Eng, 48, 2012,81–88.

[23] Feng Z. and Ivan, C.: Numerical evaluation of flow and heat transfer in plate-pin fin heat sinks with various pin cross-sections, Num. Heat Trans, Part A, 60 (2), 2011, 107–128.

[24] Launder B. E., Spalding D. B.: The numerical computation of turbulent flows, Computer methods in applied mechanics and engineering, 3, 1974, 269–289.

[25] Patankar S. V.: Numerical heat transfer and fluid flow; Hemisphere, Washington DC, 1980.

[26] Doormal V., Raithby G. D.: Enhancement of the simple method for predicting incompressible fluid flow, Numer. Heat. Transf, 7, 1984, 147–16.